Journal of Fluorine Chemistry 144 (2012) 86–93

Contents lists available at SciVerse ScienceDirect

Journal of Fluorine Chemistry

journal homepage: www.elsevier.com/locate/fluor

Novel para-linked and CF_3-substituted poly(amide-ether-imidazole)s: Solubility, optical and thermal properties

Mousa Ghaemy *, Farshad Rahimi Berenjestanaki

Polymer Chemistry Research Laboratory, Department of Chemistry, Mazandaran University, Babolsar, Iran

ARTICLE INFO

Article history:
Received 6 May 2012
Received in revised form 3 July 2012
Accepted 25 July 2012
Available online 1 August 2012

Keywords:
Fluorinated polyamide
Direct polycondensation
Fluorinated diamine
Thermal properties
Solubility
Fluorescent

ABSTRACT

A new photoactive fluorinated diamine, 2-(4-trifluoromethylphenyl)-4,5-bis(4-(4-amino-2-trifluoromethylphenoxy)phenyl)imidazole (TFIA), was synthesized and used for preparation of novel fluorinated poly(amide-ether-imidazole)s (PAEIs) by using direct polycondensation of the diamine with various dicarboxylic acids. The resulting PAEIs were amorphous and had intrinsic viscosity [η] in the range of 0.68–0.80 dL/g. The weight average (M_w) and number average (M_n) molecular weights of one of the polymer, measured by GPC, were 18,600 g/mol and 11,500 g/mol, respectively. These polymers were readily soluble in a variety of organic solvents and formed low-colored and flexible thin films via solution casting. Their values of cut-off wavelength (λ_0) were in the range of 380–390 nm, and all PAEIs films exhibited high optical transparency. According to thermal analysis, these polymers exhibited glass transition temperatures (T_g)s in the range of 160–250 °C, initial decomposition temperature (T_i) from 295 to 400 °C and temperature of 10% weight loss ($T_{10\%}$) from 400 to 490 °C in N_2. These polymers exhibited strong UV–vis absorption at 310 nm in solution and in films and their fluorescence emission peaks appeared around 430–520 nm with the quantum yields in solution varied from 10% to 29%.

1. Introduction

The chemistry of aromatic polyamides has undergone outstanding developments in the last few years to overcome the problem of processability due to their high glass-transition and melting temperature [1,2]. Many novel diamine or diacid monomers have been specially designed using different approaches, such as incorporation of flexible or bridging functional groups [3–6], bulky pendant groups [7–11], cardo groups [12–14], heterocyclic rings [15,16] and meta- or ortho-catenated as a less symmetric aromatic units [17–19] to afford the success in preparation of organosoluble polyamides. Recently, considerable attention has been devoted to the synthesis of fluorine containing polymers. Incorporation of the bulky fluorine groups serves to increase the free volume of the polymers, thereby improving some properties such as solubility, gas permeability, optical transparency and flame resistance [20–23]. In addition, it also reduces the moisture absorption, crystallinity, dielectric constant and color. Imidazole ring is a useful n-type building block with high-electron affinity and good thermal stability and has been successfully incorporated in small molecules and polymers as the electron-transport component of OLEDs [24–30].

This study explores the synthesis and basic characterization of several novel poly(amide-ether-imidazole)s having imidazol-trifluoromethyl moieties as well as aryl-ether unit in their backbone. These PAs were prepared by direct polycondensation of a new synthesized diamine, 2-(4-trifluoromethylphenyl)-4,5-bis(4-(4-amino-2-trifluoromethylphenoxy)phenyl) imidazole (TFIA), with various aromatic and aliphatic dicarboxylic acids. TFIA and the intermediates were characterized by mass, FT-IR, ^1H and ^{13}C NMR spectroscopy, and elemental analysis. The obtained PAEIs were characterized by FT-IR, H NMR, elemental analysis and viscosity measurements and their properties such as organosolubility, thermal and photophysical are investigated and discussed.

2. Experimental

2.1. Materials

All materials and solvents were purchased either from Merck or from Fluka Chemical Co. 4-(Trifluoromethyl)benzaldehyde, 2-chloro-5-nitrobenzotrifluoride, 4,4′-dimethoxybenzil, ammonium acetate, hydrazine monohydrate, 10% Pd/C, potassium carbonate, triphenyl phosphite (TPP), acetic acid, and all dicarboxylic acids, and solvents such as dimethylformamide (DMF), dimethylsulfoxide (DMSO), ethanol, methanol, acetone, hexamethylphosphoramide (HMPA), and tetrahydrofuran (THF) were used without further purification. N-methyl-2-pyrrolidone (NMP), N,N-dimethylacetamide (DMAc), and pyridine were purified by distillation over

* Corresponding author. Tel.: +98 112 534 2353; fax: +98 112 534 2302.
E-mail address: ghaemy@umz.ac.ir (M. Ghaemy).

0022-1139/$ – see front matter © 2012 Elsevier B.V. All rights reserved.
http://dx.doi.org/10.1016/j.jfluchem.2012.07.014

calcium hydride under reduced pressure. LiCl and $CaCl_2$ were dried at 180 °C in vacuum for 14 h.

2.2. Measurements

FT-IR measurements were performed on a Bruker-IFS48 spectrometer (Ettlingen, Germany). The spectra of solids were obtained using KBr pellets. ^{1}H NMR and ^{13}C NMR spectra were recorded in dimethyl sulfoxide-d_6 (DMSO-d_6) solution using a Bruker Avance 400 MHz instrument (Germany), operated at 500 MHz for proton and 100 MHz for carbon using DMSO-d_6, and tetramethylsilane was used as an internal standard. Elemental analysis was run in a Flash EA 1112 series analyzer. Melting points were determined in open capillaries with IA 9200 Series Digital Melting Point apparatus. Differential scanning calorimetry (DSC) and thermogravimetric (TGA) analyses were recorded on a Stanton Redcraft STA-780 (London, UK) at heating rate of 10 °C/min under N_2 atmosphere. Glass transition temperatures (T_g)s were read at the middle of the transition in the heat capacity and were taken from the second heating scan after quick cooling from 350 °C at a cooling rate of 200 °C/min. Intrinsic viscosity [η] were measured using an Ubbelohde viscometer with polymer solutions in DMAc at 30 °C. To determine the values of [η], at first three viscosity numbers (η_{red}) were measured at concentrations of 0.10, 0.25, and 0.50 g/dL in DMAc. These viscosity numbers were plotted against the concentrations used, and then the linear extrapolation was done. The values of [η] were determined as the *y*-axis intersect. UV–vis absorption and fluorescence emission spectra were recorded in NMP solution and in polymer films on a Cecil 5503 and Perkin-Elmer LS-3B spectrophotometers, respectively. Also, cut-off wavelength (absorption edge) values (λ_0) of the prepared thin films were determined. Weight and number-average molecular weights of the one of the resulting PAs were determined by gel-permeation chromatography (GPC). This chromatography was performed on a Waters 150-C instrument using Styragel columns and a differential refractometer detector. The molecular weight calibration was carried out using polystyrene standards. Calibration and measurements were made at a flow rate of 1 mL/min with THF as the eluent. Mass measurements of the synthesized compounds were performed on a Bruker-BiFlex III MALDI-TOF spectrophotometer (Bruker Daltonics, Billerica, MA).

2.3. Synthesis

The synthetic procedures for the synthesis of target diamine are reported below and shown in Scheme 1.

2.4. 4,4′-Dihydroxybenzil (BHD)

A mixture of 4,4′-dimethoxybenzil (2.50 g, 0.0092 mol), glacial acetic acid (25 mL), and HBr (30 mL) was refluxed for 12 h under N_2. After cooling, 5 mL HBr was added and mixture was refluxed for another 12 h. Upon completion of the reaction (as witnessed by TLC), the medium was poured into 200 mL deionized water. The organic product was extracted with 220 mL ethyl acetate. The organic phase was thoroughly washed with water in order to remove all acids and then dried over magnesium sulfate. The product was obtained as crystal after evaporation of the solvent in a rotary evaporator. The yield after drying in a vacuum oven at 80 °C was 90% (1.79 g) with melting point of 120 °C. FT-IR (KBr, cm^{-1}): 3031 (OH stretching), 1633 (C=O stretching), 1612 (C=C stretching), 1226 (C–O–C stretching). ^{1}H NMR (400 MHz, DMSO-d_6): δ = 10.84 (2H OH, s), 6.91–7.77 (8H, m) ppm. $C_{14}H_{10}O_4$: calculated C, 69.42%; H, 4.13%; N, 0%; found C, 69.38%; H, 4.16%; N, 0%. *m*/*e*: 242.06, 243.06, 244.06.

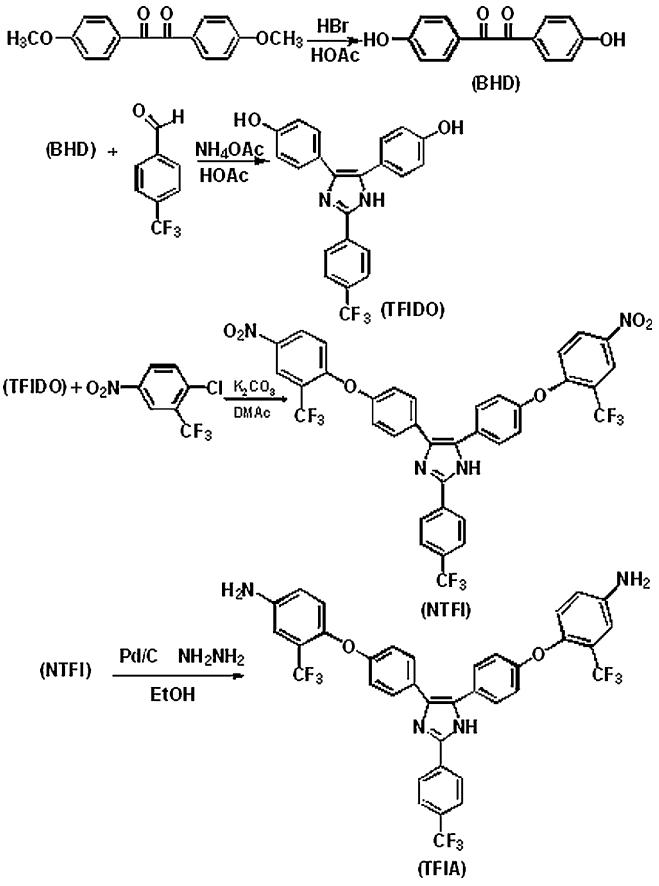

Scheme 1. Synthesis of target diamine TFIA.

2.5. 2-(4-(Trifluoromethyl)phenyl)-4,5-bis(4-hydroxyphenyl) imidazole (TFIDO)

A mixture of 4-(trifluoromethyl)benzaldehyde (1.00 g, 0.0057 mol), BHD (1.39 g, 0.0057 mol), ammonium acetate (3.18 g, 0.041 mol) and 20 mL glacial acetic acid was refluxed for 24 h under N_2. On cooling, the white precipitate was collected by filtration, washed with ethanol and dried in vacuum oven at 80 °C. The yield was 89% (2.10 g) with a melting point of 150 °C. FT IR (KBr, cm^{-1}): 3031 (OH stretching), 1614 (C=N stretching), and 1521 (C=C stretching), 1252 (C–O–C stretching).^{1}H NMR (400 MHz, DMSO-d_6): δ = 12.69 (1H NH, s), 9.67 (1H OH, s), 9.37 (1H OH, s), 8.25 (2H, d, *J* = 8 Hz), 7.81 (2H, d, *J* = 8 Hz), 7.35 (4H, dd, *J* = 4 Hz), 6.69 (4H, dd, *J* = 4 Hz) ppm. $C_{22}H_{15}F_3N_2O_2$: calculated C, 66.66%; H, 3.78%; N, 7.07%; found C, 66.63%; H, 3.81%; N, 7.04%. *m*/*e*: 396.11, 397.11, 398.12.

2.6. 2-(4-Trifluoromethylphenyl)-4,5-bis(4-(4-nitro-2-trifluoromethylphenoxy)phenyl)imidazole (NTFI)

A mixture of TFIDO (1.00 g, 0.0025 mol), 2-chloro-5-nitrobenzotrifluoride (1.127 g, 0.005 mol), potassium carbonate (1.40 g, 0.01 mol) and N, N-dimethyl acetamide (DMAc, 15 mL) was refluxed for 8 h under N_2, and then was poured into methanol/water (1:1, v/v). The crude product was recrystallized from glacial acetic acid and dried in a vacuum oven at 80 °C. The yield was 93% (1.80 g) with a melting point of 159 °C. FTIR (KBr, cm^{-1}): 1522, 1328(–NO_2), 1254 (C–O–C stretching) and 1621 (C=N stretching). ^{1}H NMR (400 MHz, DMSO-d_6): δ = 8.50–8.52 (2H, dd, *J* = 8 Hz), 8.48–8.48 (2H, d, *J* = 2.7 Hz), 8.26–8.28 (2H, d, *J* = 8.4 Hz), 7.74–7.76 (2H, d, *J* = 8.4 Hz), 7.16–7.18 (2H, d, *J* = 8.4 Hz), 7.70–7.73 (4H, m),

7.20–7.23 (4H, m) ppm. $C_{36}H_{19}F_9N_4O_6$: calculated C, 55.81%; H, 2.45%; N, 7.23%; found C, 55.83%; H, 2.47%; N, 7.20%. *m/e*: 774.12, 775.12, 776.12, 775.11.

2.7. 2-(4-Trifluoromethylphenyl)-4,5-bis(4-(4-amino-2-trifluoromethylphenoxy)phenyl)imidazole (TFIA)

3.50 mL hydrazine monohydrate was added drop-by-drop over a 30 min period to a mixture of NTFI (2.00 g, 0.0025 mmol), 0.5 g of 10% Pd/C and 20 mL ethanol and heated for 5 h. The reaction mixture was then filtered while hot to remove Pd/C and heated to reduce the volume of solvent. After cooling, the precipitate was isolated by filtration, recrystallized from ethanol and dried in a vacuum oven at 80 °C. The yield was 89% (1.58 g) with a melting point of 200 °C. FT-IR (KBr, cm^{-1}): 3445–3318 (NH_2), 1223 (C–O–C), 1621 (C=N), and 1492(C=C). ^{1}H NMR (400 MHz, DMSO-d_6): δ = 12.89 (1H, s), 8.28 (2H, d, J = 8 Hz), 7.83 (2H, d, J = 8 Hz), 7.5 (4H, m), 6.83–6.93 (10H, m), 5.50(4H, s) ppm. ^{13}C NMR (100 MHz, DMSO-d_6): 111.0, 115.9, 116.9, 119.0, 121.6, 123.4, 123.6, 124.0, 125.3, 125.8, 126.1, 128.0, 128.9, 129.7, 129.9, 130.5, 134.4, 137.3, 142.1, 142.6, 144.0, 146.2, 157.7, 158.8, 161.4, 167.6. $C_{36}H_{23}F_9N_4O_2$: calculated C, 60.50%; H, 3.22%; N, 7.84%; found C, 60.46%; H, 3.27%; N, 7.82%. *m/e*: 714.17, 715.17, 716.17, 715.16, 717.18.

3. Synthesis of PAEIs

General procedure for the preparation of PAEIs is described as follows. In a 50 mL two-necked round-bottomed flask equipped with a reflux condenser, a nitrogen gas inlet tube, and a magnetic stirrer bar, a mixture of 1 mmol (0.714 g) diamine (TFIA), 1 mmol of a dicarboxylic acid, 1.2 mL TPP, 1 mL pyridine, 0.6 g LiCl, 0.6 g $CaCl_2$ and 5.0 mL NMP was refluxed under a stream of N_2 at 120 °C for 12 h. After cooling, the obtained polymer solution was poured into a large volume of methanol giving rise to a precipitate which was washed thoroughly with hot water; it was then extracted with hot methanol using a soxhlet extractor for 10 h to remove low molecular weight fractions, and dried at 80 °C in a vacuum oven for 24 h.

PAEI-a: Yield = 90%, [η] = 0.80 dL/g. FT-IR (KBr, cm^{-1}): 3550 (N–H, imidazole), 3420 (N–H, amide), 1374 (C=N stretching) and 1227 (C–O–C). ^{1}H NMR (400 MHz, DMSO-d_6): δ = 13.65 (1H, imidazole ring), 10.76 (2H, NH amide), 6.75–8.86 (22H, aromatic protons) ppm. $[C_{44}H_{25}F_9N_4O_4]_n$: calculated C, 62.55%; H, 2.96%; N, 6.63%; found: C, 62.59%; H, 2.99%; N, 6.58%.

PAEI-b: Yield = 92%, [η] = 0.68 dL/g. FTIR (KBr, cm^{-1}): 3546 (N–H, imidazole), 3438 (N–H, amide), 1378 (C=N stretching) and 1231 (C–O–C). ^{1}H NMR (400 MHz, DMSO-d_6): δ = 13.70 (1H, imidazole ring), 10.63 (2H, NH amide), 7.09–8.57 (22H, aromatic protons) ppm. $[C_{44}H_{25}F_9N_4O_4]_n$: calculated C, 62.55%; H, 2.96%; N, 6.63%; found: C, 62.52%; H, 2.98%; N, 6.61%.

PAEI-c: Yield = 89%, [η] = 0.70 dL/g. FT-IR (KBr, cm^{-1}): 3543 (N–H, imidazole), 3494 (N–H, amide), 1398 (C=N stretching) and 1233 (C–O–C). ^{1}H NMR (400 MHz, DMSO-d_6): δ = 13.65(1H, imidazole ring), 10.63 (2H, NH amide), 7.10–8.57 (21 H, aromatic protons) ppm. $[C_{43}H_{24}F_9N_5O_4]_n$: calculated C, 60.99%; H, 2.95%; N, 8.27%; found: C, 60.95%; H, 2.97%; N, 8.25%.

PAEI-d: Yield = 90%, [η] = 0.75 dL/g. FT-IR (KBr, cm^{-1}): 3558 (N–H, imidazole), 3374 (N–H, amide), 1373 (C=N stretching) and 1239 (C–O–C). ^{1}H NMR (400 MHz, DMSO-d_6): δ = 13.09 (1H, imidazole ring), 10.45 (2H, NH amide), 6.07–7.90 (18H, aromatic protons), 1.36–1.55 (8H, aliphatic protons) ppm. $[C_{42}H_{29}F_9N_4O_4]_n$: calculated C, 61.16%; H, 3.51%; N, 6.79%; found: C, 61.19%; H, 3.57%; N, 6.74%.

PAEI-e: Yield = 91%, [η] = 0.78 dL/g. FT-IR (KBr, cm^{-1}): 3487 (N–H, imidazole), 3294 (N–H, amide), 1389 (C=N stretching), and 1229 (C–O–C). ^{1}H NMR (400 MHz, DMSO-d_6): δ = 13.04

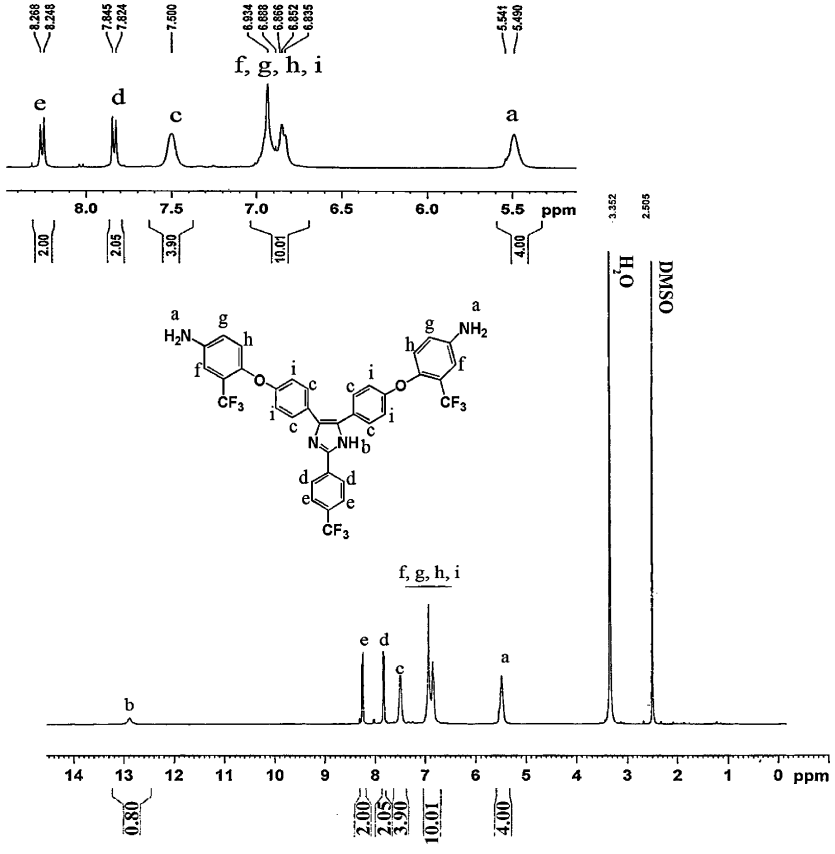

Fig. 1. ^{1}H NMR spectrum of TFIA in DMSO-d_6.

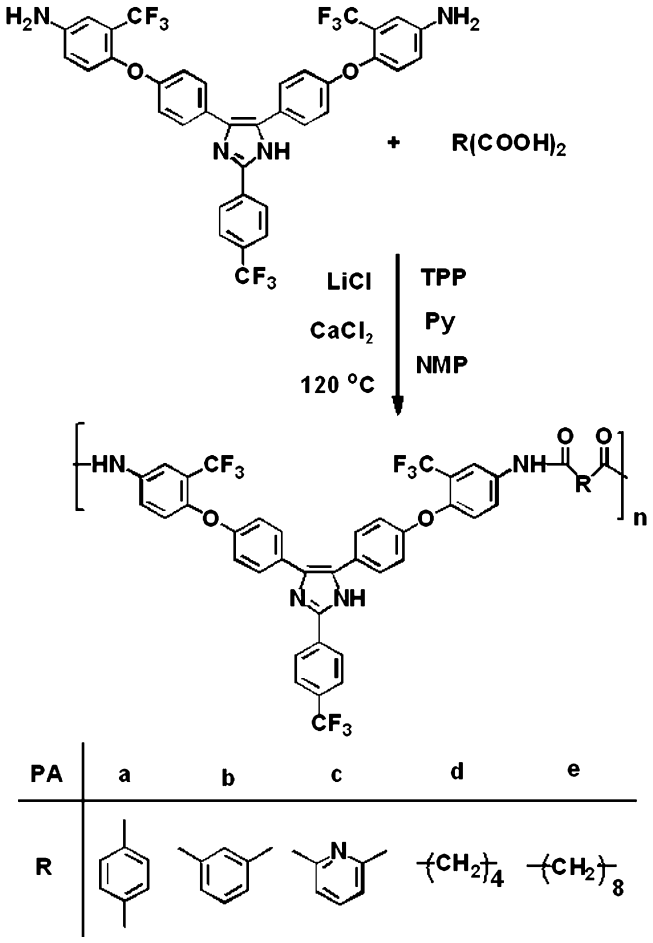

Scheme 2. Polycondensation reaction of TFIA with different dicarboxylic acids.

(1H, imidazole ring), 10.40 (2H, NH amide), 6.09–7.78 (18H, aromatic protons), 1.36–1.55 (16H, aliphatic protons) ppm. $[C_{46}H_{37}F_9N_4O_4]_n$: calculated C, 62.72%; H, 4.20%; N, 6.36%; found: C, 62.77%; H, 4.24%; N, 6.32%.

4. Results and discussion

4.1. Synthesis and characterization of diamine (TFIA)

A new aromatic diamine was synthesized according to the synthetic route depicted in Scheme 1. The preparation of BHD was carried out according to the procedure given in the literature [31]. ^{1}H NMR spectrum of BHD showed a signal at 10.84 ppm related to the phenolic hydroxyl. The reaction of BHD with 4-(trifluoromethyl)benzaldehyde in the presence of NH_4OAc in glacial acetic acid is a well known reaction for the preparation of imidazole ring [32] and has afforded the TFIDO. IR spectrum of TFIDO exhibited absorption at 1614 cm^{-1} due to C=N stretching vibration and ^{1}H NMR spectrum of this compound showed signals at 12.69 ppm and in the region of 9.67–9.37 ppm related to the N–H of imidazole ring and phenolic O–H groups, respectively. The chlorodisplacement reaction between TFIDO and 2-chloro-5-nitrobenzotrifluoride in presence of K_2CO_3 in DMAc afforded the dinitro compound NTFI. The FT-IR spectrum of NTFI showed characteristic absorption bands at 1522 cm^{-1} (NO_2 asymmetrical stretching) and 1328 cm^{-1} (NO_2 symmetrical stretching). The catalytic reduction of the nitro groups by means of Pd/C-catalyzed hydrazine monohydrate in ethanol afforded the target diamine. FT-IR spectrum of the diamine (TFIA) showed the characteristic absorption bands of the primary amine at 3318 and 3445 cm^{-1} due to N–H stretching. The ^{1}H NMR spectrum of diamine showed signals at 12.89 related to the protons of NH group in imidazole ring. The ^{1}H NMR spectrum also confirmed that the nitro groups have been completely transformed into the amino groups by the high field shift of the aromatic protons and by the signal at 5.50 ppm. The ^{1}H NMR spectrum of diamine is shown with descriptions in Fig. 1. These results clearly confirmed that the diamine prepared here in is consistent with the proposed structure.

4.2. Synthesis and characterization of PAEIs

A series of novel well-oriented macromolecules containing imidazole and trifluoromethyl moieties in the backbone was synthesized based on the phosphorylation polycondensation from the diamine (TFIA) and various commercial available dicarboxylic diacids such as terephthalic acid, isophthalic acid, pyridine-2,6-dicarboxylic acid, adipic acid, and sebacic acid as shown in Scheme 2. The phosphorylation polycondensation as described for the first time by Yamazaki et al. [33] was carried out by using triphenylphosphite and pyridine as condensing agents. The polymerization readily proceeded within a homogeneous solution in NMP and in the presence of LiCl and $CaCl_2$, and afforded highly viscous polymer solutions with up to 92% yield. Since Yamazaki's development, many researchers have utilized the activated polyamidation using the TPP activator and found that the addition of a small amount of LiCl or $CaCl_2$ enhances the molecular weight of the polyamides. The intrinsic viscosity [η] values of the prepared polymers in DMAc at 25 °C as well as the results of GPC analyses for PAEI-e are tabulated in Table 1. The [η] values for all polymer solutions were determined through the extrapolation of the concentrations used to zero [33]. The obtained polymers had limited viscosity numbers in the range of 0.68–0.80 dL/g. The average molecular weights of these polymers, except PAEI-e, were not detectable by GPC because of their insolubility in THF eluent. The weight average (M_w) and number average (M_n) molecular weights of the PAEI-e were 18,600 g/mol and 11,500 g/mol, respectively, high enough to obtain flexible and tough thin films by casting from their DMF solutions. The structures of the PAs were confirmed by means of

Table 1
Solubility behavior of PAEIs.

Polymer	[η][a], dL/g	M_n, g/mol[b]	M_w, g/mol[b]	DMAc	DMF	NMP	DMSO	Py	THF	Methanol	HMPA
PAEI-a	0.80	–	–	++	++	++	++	++	–+	––	++
PAEI-b	0.68	–	–	++	++	++	++	++	–+	––	++
PAEI-c	0.70	–	–	++	++	++	++	++	–+	–	++
PAEI-d	0.75	–	–	++	++	++	++	++	–+	–	++
PAEI-e	0.78	11,500	18,600	++	++	++	++	++	++	––	++

The solubility was determined by using 5 g sample in 100 mL of solvent.
Abbreviations: DMAc, N,N-dimethyl acetamide; DMF, N,N-dimethyl formamide; NMP, N-methyl pyrrolidone; DMSO, dimethyl sulfoxide; THF, tetrahydrofuran; Py, pyridine; HMPA, hexamethylphosphoramide; ++: soluble at room temperature; –+: soluble on heating at 60 °C; ––: insoluble on heating at 60 °C.
[a] Measured in DMAc at 25 °C.
[b] Measured by GPC in THF with polystyrene as a standard.

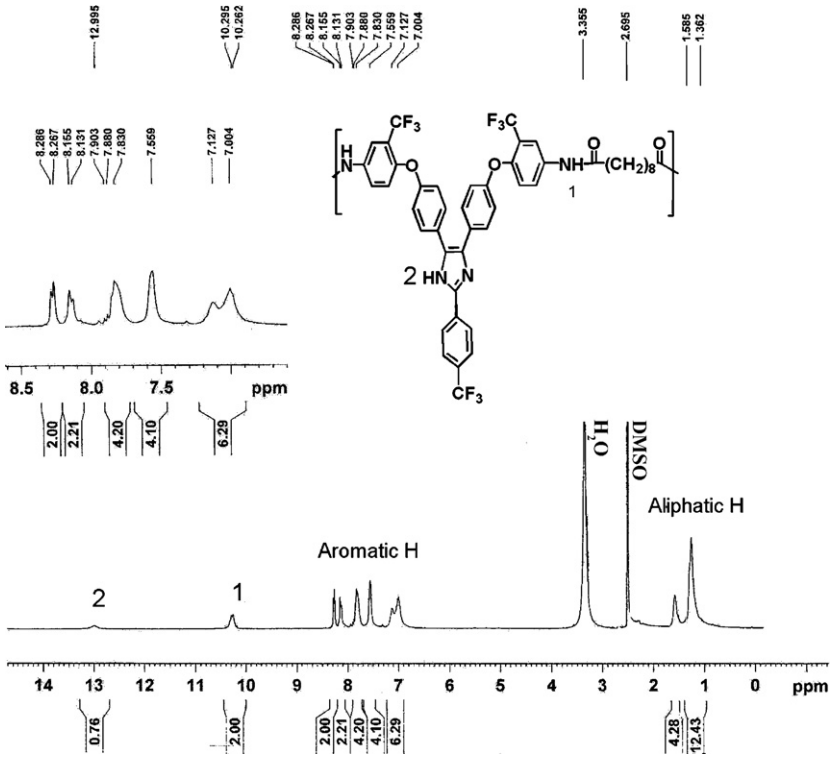

Fig. 2. ^{1}H NMR spectrum of PAEI-e in DMSO-d_6.

FT-IR and ^{1}H NMR spectroscopy methods. In general, FT-IR spectra of the PAs showed the characteristic absorption bands around 3550 (N–H imidazole, stretching), 3370 (N–H amide, stretching), 1630 (C=O stretching), 1375 (C=N stretching of imidazole ring) and around 1227 cm^{-1} (C–O stretching). The ^{1}H NMR spectra of the resulting PAEIs a signal appeared at the most downfield region, in the range of 13.04–13.70 ppm, can be attributed to the proton of imidazole ring and in the range of 10.76–10.40 is related to the protons of amide linkages. In addition to the signals in the region of 7.10–8.78 ppm related to the aromatic protons, PAEI-d and PAEI-e also showed signals in the range of 3.83–3.93 and 1.36–1.55 ppm, respectively, related to the aliphatic protons. Assignment of protons in the spectra is consistent with the proposed chemical structure of polymers. The ^{1}H NMR spectrum of the representative polymer, PAEI-e, is shown in Fig. 2.

5. Properties of PAEIs

5.1. Solubility

The solubility behavior of the prepared PAEIs was tested qualitatively in various organic solvents at 5% (w/v), and the results are summarized in Table 1. All the prepared PAEIs exhibited excellent solubility in polar aprotic solvents such as NMP, DMAc, DMF, DMSO, HMPA and pyridine at room temperature and in less polar solvent such as THF at 60 °C. The good solubility of these PAEIs should be the result of the introduction of the bulky phenyl pendant with trifluoromethyl substitutes in polymer backbone. When the CF_3-substituted diamine TFIA is polymerized with various aliphatic and aromatic dicarboxylic acids, the corresponding PAEIs with ortho- and para-oriented CF_3 moieties per repeat unit would be an exceptional material from the solubility point of view. Dense packing of the polymer chains was probably disturbed by the bulky CF_3 and phenyl containing-CF_3 groups attached to the main chains along with a good path in the direction of the bonds in the macromolecular backbones which led to the increased chain distances and decreased chain interactions; consequently, the solvent molecules were able to penetrate more easily into the polymer chains and interact with the polar linkages of the PAEIs backbone such as imidazole ring, ether and amide linkages. Therefore, the presence of polar CF_3 pendants and ether and imidazole units in the main chains can contribute effectively in the solubility of these PAEIs as compared with the solubility of the previously reported polyamides [34,35]. These polymers can be processed into thin colorless films by casting from their solutions. The ease of solubility varies depending upon the dicarboxylic acids used. The PAEI-e synthesized from sebacic acid with longer aliphatic unit exhibited better solubility behavior in THF in comparison with the other PAEIs.

Table 2
Photophysical properties of TFIA and PAEIs.

Polymer	$\lambda_{a.max}$ (nm)		$\lambda_{e.max}$ (nm)		Φ_f (%)[c]
	Solution[a]	Film[b]	Solution[a]	Film[b]	
PAEI-a	339	342	520	522	9
PAEI-b	337	339	502	509	10
PAEI-c	325	328	489	492	22
PAEI-d	310	315	452	455	20
PAEI-e	307	–309	445	450	24
TFIA	305	–	405	–	34

$\lambda_{a.max}$ = maximum absorption wavelength. $\lambda_{e.max}$ = maximum emission wavelength. The excitation wavelength was 320 nm.

[a] Polymer concentration of 0.2 g/dL in NMP.

[b] PAEIs thin films were made by dissolving about 0.5 g of the PAEI in 5 mL of NMP, and the homogeneous solution in a glass culture dish was heated under vacuum in three steps: at 50 °C for 1 h, 100 °C for 2 h, and 150 °C for 5 h. Polymer films were self-stripped off from the glass surface by soaking in water. The polymer films were further dried in vacuum oven at 170 °C for 10 h.

[c] Fluorescence quantum yield relative to 0.1 N quinine sulfate in 1 N H_2SO_4 (aq) (Φ_f = 0.55) as a standard.

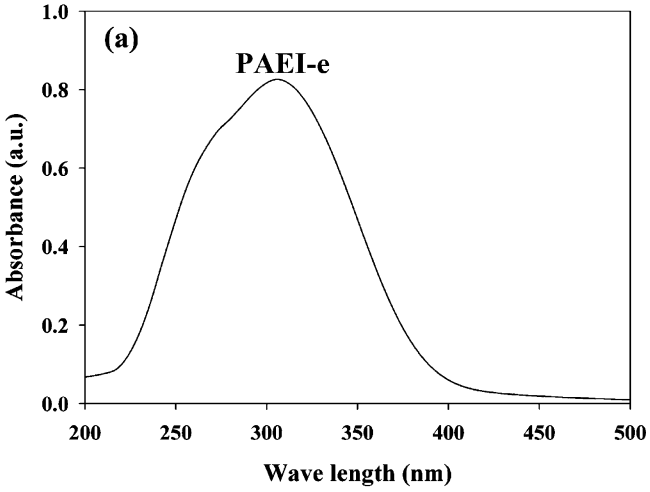

Fig. 3. Absorption (a) and transmission (b) spectra of PAEIe film.

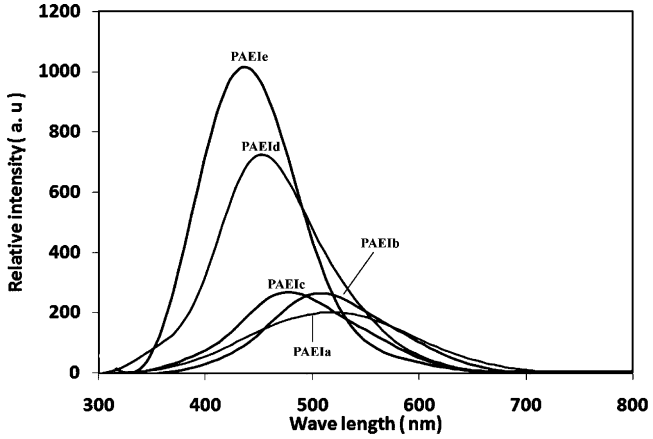

Fig. 4. Fluorescence emission spectra of PAEIs.

5.2. Optical properties

To prepare crack-free and homogeneous thin films for the measurement of optical properties, solutions of PAEIs were made by dissolving about 0.5 g of the PAEI in 5 mL of NMP to afford an approximate 10 wt.% solution. The homogeneous solution was poured into a 9-cm diameter glass culture dish, which was heated under vacuum at 50 °C for 1 h, 100 °C for 2 h, and 150 °C for 5 h to evaporate the solvent slowly. Polymer films were self-stripped off from the glass surface by soaking in water. The polymer films were further dried in vacuum oven at 170 °C for 10 h. The photophysical properties of the diamine (10^{-5} M) and PAEIs (0.2 g/dL) in dilute NMP solutions were investigated by UV–vis and fluorescence spectroscopy. Table 2 lists some important optical data obtained from dilute solutions of the diamine and PAEIs in NMP and from thin films of PAEIs. The TFIA showed strong UV absorption with maximum at $\lambda_{a.max}$ = 298–305 nm. The absorption spectra of the resulting PAEIs in solutions and in films were nearly identical with each other. The maximum absorption wavelength ($\lambda_{a.max}$) of all PAEIs appeared in the range of 310–320 nm, which shows a relatively small energy band gap for $\pi \rightarrow \pi^*$ transition. Fig. 3 shows molar absorptivity spectrum of the representative polymer, PAEI-e, film (top) and UV–vis transmission spectrum of the same polymer film (bottom). The plateau region of the light transmittance in the UV–vis spectrum was extended to about 800 nm, indicating high degree of the film transparency. Moreover, the λ_0 values (absorption edge or cut-off wavelength) of the resulting polymers were found to be in the range of 380–390 nm. In these polymers, the presence of CF_3 groups in the structure of the repeating units plays the main role in its excellent optical behavior. By inducing separation of the macromolecular chains caused by $-CF_3$ and bulky phenyl groups, the formation of charge transfer complex, which imparts deep color to the polymer, is largely hindered, and thus the color intensity is considerably reduced. Generally, the results obtained clearly show that the prepared thin films have low color intensity and high level of optical transparency in the UV–vis light region.

To investigate the emission properties of TFIA and PAEIs, an excitation wavelength of 320 nm was used in all cases. The TFIA showed strong blue fluorescent light in dilute (10^{-5} M) NMP solution with maximum emission wavelength at $\lambda_{e.max}$ = 415 nm. Photoluminescence (PL) spectra of the PAEI-a, PAEI-d, PAEI-e (0.2 g/dL) and TFIA (10^{-5} M) in dilute NMP solutions are shown in Fig. 4. To measure the PL quantum yields (Φ_f), dilute polymer solutions (0.2 g/dL) in NMP were prepared. A 0.1 N solution of quinine in H_2SO_4 (Φ_f = 0.55) was used as reference according to the literature [28]. The fluorescence spectra of these PAEIs in NMP solutions exhibited broad emission peaks with the maxima in the range of 430–520 nm and quantum yields in the range of 9–24%. The aliphatic PAEIs, PAEI-e and PAEI-d, exhibit emission both in solution and in solid state at $\lambda_{e.max}$ = 445–455 nm with Φ_f = 20–24% and the aromatic PAEIs, PAEI (a–c), exhibited emission both in solution and in solid state at $\lambda_{e.max}$ = 490–520 nm with Φ_f = 9–22%. The blue shift and higher intensity of the photoluminescence peak of the aliphatic polyamides compared with the aromatic polyamide could be attributed to the effectively reduced conjugation and capability of charge-transfer complex formation by aliphatic diacids in comparison with the electron-donating amino unit and the strongly electron-accepting aromatic diacid unit [34–36].

5.3. Thermal properties

The thermal behavior data of these PAEIs were assessed by using DSC and TGA analysis. DSC was used to determine the glass-transition temperature values (T_gs) of the samples obtained with a heating rate of 10 °C/min under nitrogen, Fig. 5(a). The T_g values were taken as the midpoint of the change in slope of the baseline in DSC curves. The DSC curves did not exhibit endothermic peak up to 350 °C which can be associated to the amorphous nature of the PAEIs. Quenching from temperature of 350 °C to room temperature yielded amorphous samples so that in most cases the T_gs could easily be observed in the second heating traces of DSC. The amorphous nature of these PAEIs can be attributed to their bulky

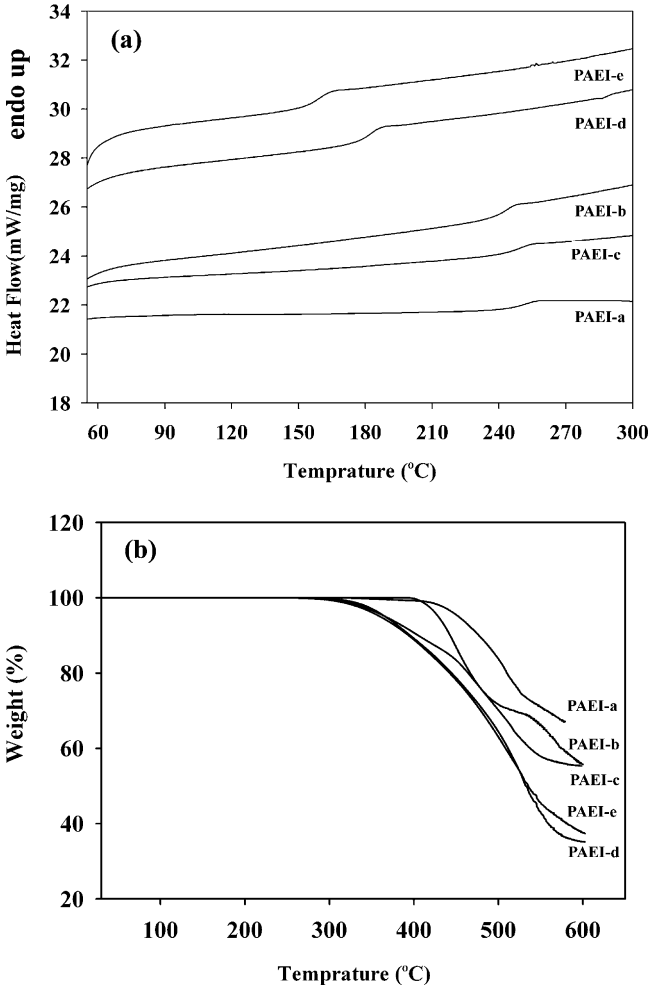

Fig. 5. DSC (a) and TGA (b) curves of PAEIs under N_2 at 10 °C/min.

pendent group which decreased the interchain interaction resulting in loose polymer chain packaging and aggregates. The T_g values of these polymers were in the range of 160–250 °C, depending on the stiffness of the residue of diacids in the polymer backbone, and the data are summarized in Table 3. In general, molecular packing and chain rigidity are among the main factors influencing on T_g values. Therefore, the increased rotational barrier caused by the bulky pendant in diamines and side chain-side chain and side chain-main chain interactions enhanced T_g values. However, T_g values of these polymers are comparable [35] and lower than T_g values of the previously reported polyamides [34] which can be due to presence of flexible ether linkages in the main chains. As anticipated, the T_g values of these PAEIs also depend on the stiffness of dicarboxylic acid component in the polymer chain and the increasing order of T_g generally correlated with that of chain rigidity. PAEIs obtained from aliphatic dicarboxylic acid such as PAEI-d and PAEI-e, showed lower T_gs of 180 °C and 160 °C, respectively, because of the presence of flexible aliphatic unit between the aromatic amide units and low rotation barrier of their diacid moieties, and the highest T_g of 250 °C was observed for PAEI-a derived from terephthalic acid because of the highest rigidity which inhibited the molecular motion.

The thermal stability of the resulting PAs was evaluated by TGA at a heating rate of 10 °C/min under nitrogen atmosphere. Fig. 5(b) presents TGA curves of the PAEIs, and corresponding initial decomposition temperatures (T_i) as well as weight loss temperatures of 10% ($T_{10\%}$) were all determined from original curves and

Table 3
Thermal characteristic data of PAEIs.

Polymer	T_g (°C)[a]	T_i (°C)	$T_{10\%}$ (°C)	C.Y. (%) at 600 °C[b]
PAEI-a	250	400	490	68
PAEI-b	242	390	460	58
PAEI-c	248	320	420	58
PAEI-d	180	300	405	37
PAEI-e	160	295	400	35

T_g, glass transition temperature; decomposition temperature, recorded via TGA at 10 °C/min under N_2 (20 cm^3/min); T_i, temperature for 0% weight loss; $T_{10\%}$, temperature for 10% weight loss.

[a] Midpoint temperature of baseline shift on the second DSC scan trace (10 °C/min, under N_2, 20 cm^3/min) of the sample after quenching from 350 °C.

[b] C.Y. = char yield: residual weight percentage at 600 °C in N_2.

listed in Table 3. The T_i and $T_{10\%}$ values of the aliphatic and aromatic PAEIs stayed within 295–400 °C and 400–490 °C, respectively, and the amount of carbonized residue (char yield) of these polymers was from 35% to 68% at 600 °C in nitrogen atmosphere, depending on the structure of diacid component, implying that these polyamides possess reasonable thermal stability. The data from thermal analysis show that the resulting polymers have fairly high thermal stability. This explains that introduction of strong electron negativity of $-CF_3$ groups might have enhanced the polarity of the polymer, which should restrict the movement of polymer-link and led to better thermal stability than previously reported polyamides [3,34].

6. Conclusion

A series of new optically active poly(amide-ether-imidazole)s containing substituted imidazole ring and ether linkages in the main chains and $-CF_3$ side groups were successfully synthesized from a new diamine monomer and various aromatic and aliphatic dicarboxylic acids via direct polycondensation method. These PAEIs exhibited excellent solubility in many polar aprotic organic solvents and capability of forming colorless flexible thin films through solution casting. Incorporating the bulky $-CF_3$ side groups linked in ortho and para positions and flexible aryl ether linkages along the symmetrically oriented chains could change their alignment, disrupting the copolanarity of aromatic rings due to local macromolecular twisting, and highly increase the organo-solubility of the polymers. Accordingly, all the polymeric low-colored thin films were significantly flexible and showed high optical transparency in the UV–vis light region. The PAEIs have also exhibited fluorescence emission with the maxima in the region of 430–520 nm in solution and in solid state due to presence of triphenyl imidazole unit in their backbones. In sum, these fluoro-containing PAEIs displayed excellent organo-solubility, good film-forming capability, reasonable thermal stability and T_g values suitable for thermoforming processing.

Appendix A. Supplementary data

Supplementary data associated with this article can be found, in the online version, at http://dx.doi.org/10.1016/j.jfluchem.2012.07.014.

References

[1] J.M. García, F.C. García, F. Serna, J.L. de la Pena, Progress in Polymer Science 35 (2010) 623–686.
[2] M. Scholl, Z. Kadlecova, H.-A. Klok, Progress in Polymer Science 34 (2009) 24–61.
[3] H. Behniafar, M. Sedaghatdoost, Journal of Fluorine Chemistry 132 (2011) 276–284.

[4] X.-L. Wang, Y.-F. Li, C.-L. Gong, T. Ma, F.-C. Yang, Journal of Fluorine Chemistry 129 (2008) 56–63.
[5] J.F. Espeso, E. Ferrero, J.G. de la Campa, A.E. Lozano, J. de Abajo, Journal of Polymer Science Part A: Polymer Chemistry 39 (2001) 475–485.
[6] V. Calderon, F.C. Garcia, J.L. De La Pena, E.M. Maya, J.M. Gercia, Journal of Polymer Science Part A: Polymer Chemistry 44 (2006) 2270–2281.
[7] G.S. Liou, S.H. Hsiao, M. Ishida, M. Kakimoto, Y. Imai, Journal of Polymer Science Part A: Polymer Chemistry 40 (2002) 1781–1789.
[8] G.S. Liou, S.H. Hsiao, Journal of Polymer Science Part A: Polymer Chemistry 41 (2003) 94–105.
[9] E.M. Maya, A.E. Lozano, J.G. de la Campa, J. de Abajo, Macromolecular Rapid Communications 25 (2004) 592–597.
[10] S.H. Hsiao, C.W. Chen, G.S. Liou, Journal of Polymer Science Part A: Polymer Chemistry 42 (2004) 3302–3313.
[11] N. San-Jose, A. Gomez-Valdemoro, F.C. Garcia, F. Serna, J.M. Garcia, Journal of Polymer Science Part A: Polymer Chemistry 45 (2007) 4026–4036.
[12] D.J. Liaw, B.Y. Liaw, C.M. Yang, Macromolecules 32 (1999) 7248–7250.
[13] C.P. Yang, J.A. Chen, Polymer International 49 (2000) 103–109.
[14] G.S. Liou, H.J. Yen, Y.T. Su, H.Y. Lin, Journal of Polymer Science Part A: Polymer Chemistry 45 (2007) 4352–4363.
[15] A.D. Sagar, R.D. Shingte, P.P. Wadgaonkar, M.M. Salunkhe, European Polymer Journal 37 (2001) 1493–1498.
[16] R.R. Pal, P.S. Patil, M.M. Salunkhe, P.P. Wadgaonkar, N.N. Maldar, Polymer International 54 (2005) 569–575.
[17] O. Haba, H. Seino, K. Aoki, K. Iguchi, M. Ueda, Journal of Polymer Science Part A: Polymer Chemistry 36 (1998) 2309–2314.
[18] I. Sava, M. Bruma, Macromolecular Symposium 239 (2006) 36–42.
[19] I. Sava, M. Bruma, I. Ronova, High Performance Polymers 16 (3) (2004) 435–446.
[20] M.G. Dhara, S. Banerjee, Progress in Polymer Science 35 (2010) 1022–1077.
[21] D.J. Liaw, F.C. Chang, Journal of Polymer Science Part A: Polymer Chemistry 42 (2004) 5766–5774.
[22] J. Vargas, A. Martınez, A.A. Santiago, M.A. Tlenkopatchev, R. Gavinob, M. Aguilar-Vega, Journal of Fluorine Chemistry 130 (2009) 162–168.
[23] D.W. Smith, Handbook of Fluoropolymer Science and Technology, Hoboken, NJ, John Wiley & Sons, 2009.
[24] K. Mullen, Organic Light Emitting Devices: Synthesis, Properties and Applications, Wiley–VCH, Weinheim, Germany, 2006.
[25] J.A. Mikroyannidis, D. Panayiotis, V.I. Panayiotis, K. Spiliopoulos, Synthetic Metals 145 (2004) 87–93.
[26] X.H. Zhou, J.C. Yan, J. Pei, Macromolecules 37 (2004) 7078–7080.
[27] Y. Pan, X. Tang, L. Zhu, Y. Huang, European Polymer Journal 43 (2007) 1091–1095.
[28] K. Feng, F.L. Hsu, D. Van Der Veer, K. Bota, R. Xiu, Journal of Photochemistry and Photobiology A: Chemistry 165 (2004) 223–228.
[29] G. Hadjikallis, S.C. Hadjiyannakou, M. Vamvakaki, C.S. Patrickios, Polymer 43 (2002) 7269–7273.
[30] Y. Pan, X. Tang, European Polymer Journal 44 (2008) 408–414.
[31] F. Yang, J. Zhao, Y. Li, European Polymer Journal 45 (2009) 2053–2059.
[32] M. Ghaemy, S.M. Amini Nasab, Reactive and Functional Polymers 70 (2010) 306–313.
[33] D. Braun, H. Cherdron, M. Rehahn, H. Ritter, B. Voit, Polymer Synthesis: Theory and Practice; Fundamentals, Methods, Experiments, 4th ed., Springer Verlag, Berlin/Heidelberg, 2005, pp. 104–112.
[34] M. Ghaemy, R. Alizadeh, Reactive and Functional Polymers 71 (2011) 425–432.
[35] M. Ghaemy, F. Hashemi Nasr, R. Alizadeh, M. Taghavi, Macromolecular Research 20 (2012) 614–622.
[36] G.S. Liou, C.W. Chang, Macromolecules 41 (2008) 1667–1674.